

Scarless Genome Editing and Stable Inducible Expression Vectors for *Geobacter sulfurreducens*

Chi Ho Chan,^a Caleb E. Levar,^{a,b} Lori Zacharoff,^{a,c} Jonathan P. Badalamenti,^a Daniel R. Bond^{a,b}

BioTechnology Institute,^a Department of Microbiology,^b and Department of Biochemistry, Molecular Biology, and Biophysics,^c University of Minnesota-Twin Cities, Saint Paul, Minnesota, USA

Metal reduction by members of the *Geobacteraceae* is encoded by multiple gene clusters, and the study of extracellular electron transfer often requires biofilm development on surfaces. Genetic tools that utilize polar antibiotic cassette insertions limit mutant construction and complementation. In addition, unstable plasmids create metabolic burdens that slow growth, and the presence of antibiotics such as kanamycin can interfere with the rate and extent of *Geobacter* biofilm growth. We report here genetic system improvements for the model anaerobic metal-reducing bacterium *Geobacter sulfurreducens*. A motile strain of *G. sulfurreducens* was constructed by precise removal of a transposon interrupting the *fgrM* flagellar regulator gene using SacB/sucrose counterselection, and Fe(III) citrate reduction was eliminated by deletion of the gene encoding the inner membrane cytochrome *imcH*. We also show that RK2-based plasmids were maintained in *G. sulfurreducens* for over 15 generations in the absence of antibiotic selection in contrast to unstable pBBR1 plasmids. Therefore, we engineered a series of new RK2 vectors containing native constitutive *Geobacter* promoters, and modified one of these promoters for VanR-dependent induction by the small aromatic carboxylic acid vanillate. Inducible plasmids fully complemented $\Delta imcH$ mutants for Fe(III) reduction, Mn(IV) oxide reduction, and growth on poised electrodes. A real-time, high-throughput Fe(III) citrate reduction assay is described that can screen numerous *G. sulfurreducens* strain constructs simultaneously and shows the sensitivity of *imcH* expression by the vanillate system. These tools will enable more sophisticated genetic studies in *G. sulfurreducens* without polar insertion effects or need for multiple antibiotics.

Methods to remove, replace, and control genes are instrumental to understanding bacterial physiology. Together with DNA synthesis and high-throughput sequencing, these tools enable synthetic reconstruction of pathways and design of biological circuitry (1). Many genetic approaches were first developed in fast-growing bacteria such as *Escherichia coli*, while genetic techniques able to interrogate the physiology of slower-growing anaerobic organisms are often more limited (2). In some cases, heterologous expression of foreign genes can help infer function in a genetically intractable organism (3), but model hosts can lack key biochemical processes or cofactors making functional expression challenging (4). Electron transfer to metals and electrodes by *Geobacter sulfurreducens* is an example of a complex respiratory strategy encoded in multigene loci throughout the chromosome, requiring cytochrome maturation, protein secretion, cell surface attachment, sensing, and motility (5–8). The genetic study of metal reduction will ultimately require deletion and reexpression of multiple genes in the native organism, under a variety of planktonic and long-term biofilm growth conditions.

A gene replacement protocol using electroporation of linear DNA fragments was first developed for *G. sulfurreducens* in 2001 (9), and insertion of antibiotic cassettes allowed for construction of multiple deletion mutants, such as the $\Delta omcB::cat$ $\Delta omcST::nptII$ $\Delta omcE::aacC$ $\Delta omcZ::aadA$ quintuple deletion mutant. However, due to the finite number of resistance genes available in *Geobacter*, it is difficult to delete additional loci or complement such complex constructs (10). Conjugal plasmid transfer from an *Escherichia coli* donor strain, and transposon mutagenesis via nonreplicating plasmids is also feasible in *G. sulfurreducens* (9, 11). These tools accelerate mutant construction and discovery, but issues of transposon insertion polarity, growth inhibition due to use of multiple antibiotics, and unknown expression levels from pro-

motors on plasmids limit complementation and interpretation of results (12, 13). A *cre-lox* recombination gene disruption strategy used in *G. metallireducens* and *G. sulfurreducens* removes the antibiotic cassette from the chromosome (14, 15). However, this method leaves a *loxP* scar sequence and creates multiple identical *loxP* sequences throughout the genome if additional deletions are constructed (16).

In this study, we implemented a SacB/sucrose counterselection strategy to generate scarless deletions in *G. sulfurreducens*. We also tested the stability and the effect of commonly used broad-host-range plasmids on growth using soluble, insoluble, and poised electrode electron acceptors. New vectors based on the RK2 origin of replication with native constitutive and engineered inducible promoters were constructed for controlled gene expression in *G. sulfurreducens* using different electron acceptors. To accelerate the screening of constructs and promoters, we describe a real-time, high-throughput Fe(III) citrate reduction assay to measure the

Received 17 June 2015 Accepted 29 July 2015

Accepted manuscript posted online 7 August 2015

Citation Chan CH, Levar CE, Zacharoff L, Badalamenti JP, Bond DR. 2015. Scarless genome editing and stable inducible expression vectors for *Geobacter sulfurreducens*. *Appl Environ Microbiol* 81:7178–7186. doi:10.1128/AEM.01967-15.

Editor: F. E. Löffler

Address correspondence to Daniel R. Bond, dbond@umn.edu.

Copyright © 2015, Chan et al. This is an open-access article distributed under the terms of the [Creative Commons Attribution-Noncommercial-ShareAlike 3.0 Unported license](https://creativecommons.org/licenses/by-nc-sa/4.0/), which permits unrestricted noncommercial use, distribution, and reproduction in any medium, provided the original author and source are credited.

doi:10.1128/AEM.01967-15

TABLE 1 Strains and plasmids used in this study

| Strain or plasmid | Description or relevant genotype | Source or reference |
|----------------------------------|--|------------------------------|
| Strains | | |
| <i>G. sulfurreducens</i> strains | | |
| DB789 | $\Delta imcH$ | This study |
| DB1004 | $\Delta GSU0299$ | This study |
| <i>E. coli</i> strains | | |
| S17-1 | <i>recA pro hsdR RP4-2-Tc::Mu-Km::Tn7</i> | 31 |
| BW29427 (WM3064) | <i>thrB1004 pro thi rpsL hsdS lacZ</i> Δ M15 RP4-1360 Δ (<i>araBAD</i>)567 Δ <i>dapA1341::[erm pir]</i> | K. Datsenko and B. L. Wanner |
| Plasmids | | |
| Complementation vectors | | |
| pSRK-Km | pBBR1 origin, <i>oriT lacI nptII</i> | 24 |
| pRVMCS-2 | RK2 origin, <i>oriT, vanR P_{vanA}-MCS nptI bla</i> | 25 |
| pRK2-Geo1 | RK2 origin, <i>oriT, P_{acpP}-MCS nptI bla</i> | This study |
| pRK2-Geo2 | RK2 origin, <i>oriT, P_{acpP}-MCS nptI</i> | This study |
| pRK2-Geo2i | RK2 origin, <i>oriT, P_{GSU0800-vanR, P_{acpP}-MCS nptI}</i> | This study |
| pRK2-Geo5 | RK2 origin, <i>oriT, P_{taclac}-MCS, nptI</i> | This study |
| SacB suicide vectors | | |
| pSMV3 | | 32 |
| pK18mobsacB | | 31 |
| pDGSU0299 | Flanking regions of GSU0299 in pSMV3 | This study |
| pDImcH1 | Flanking regions of <i>imcH</i> in pSMV3 | This study |
| pDImcH2 | Flanking regions of <i>imcH</i> in pK18mobsacB | This study |
| ImcH vectors | | |
| pImcH4 | <i>imcH</i> in pSRK-Km | This study |
| pImcH15 | <i>imcH</i> in pRK2-Geo2 | This study |
| pImcH16 | <i>imcH</i> in pRK2-Geo2i | This study |
| pImcH17 | <i>imcH</i> in pRK2-Geo5 | This study |

response of the engineered promoter system. These new tools make it possible to construct multigene deletions, promoter modifications, in-frame fusions, and inducible genetic circuitry in *Geobacter sulfurreducens*.

MATERIALS AND METHODS

Growth and medium conditions. All strains and plasmids used in the present study are listed in Table 1. *Geobacter sulfurreducens* strains were cultured at 30°C in anoxic liquid basal minimal medium with 20 mM acetate as the electron donor and 40 mM fumarate, 50 mM ferric citrate, or 20 mM Mn(IV) oxide as the electron acceptor in sealed anaerobic tubes with a N₂:CO₂ (80:20) headspace. Basal medium was composed of 0.38 g/liter KCl, 0.2 g/liter NH₄Cl, 0.069 g/liter NaH₂PO₄·H₂O, 0.04 g/liter CaCl₂·2H₂O, and 0.2 g/liter MgSO₄·7H₂O. Basal medium also contained 10 ml/liter of a chelated mineral mix (composed of 1.5 g of nitrilotriacetic acid (NTA), 0.1 g/liter MnCl₂·4H₂O, 0.5 g/liter FeSO₄·7H₂O, 0.17 g/liter CoCl₂·6H₂O, 0.1 g/liter ZnCl₂, 0.03 g/liter CuSO₄·5H₂O, 0.005 g/liter AlK (SO₄)₂·12H₂O, 0.005 g/liter H₃BO₃, 0.09 g/liter Na₂MoO₄, 0.05 g/liter NiCl₂, 0.02 g/liter NaWO₄·2H₂O, and 0.10 g/liter Na₂SeO₄). For media containing Fe(III) citrate or Mn(IV) oxide, a nonchelated mineral mix was used in which NTA was omitted and all components were first dissolved in 50 ml of 1 N HCl. The pH of the medium was adjusted to 6.8 after the addition of all donors and acceptors, buffered with 2 g/liter NaHCO₃, purged with N₂:CO₂ gas (80:20) passed over a heated copper column to remove trace oxygen, and autoclaved for 30 min at 121°C. Liquid growth with fumarate was measured as the optical density at 600 nm (OD₆₀₀) in Balch tubes. Agar (1.5%) was added to the acetate-fumarate medium containing Trypticase peptone (0.1%) and cysteine (1 mM) when cultured on semisolid surface in an anaerobic workstation 500 (Don Whitley) with a H₂:CO₂:N₂ (5:20:75) atmosphere. Motility was assayed in acetate-fumarate medium containing 0.4% agar.

Growth with Fe(III) citrate was correlated to the amount of Fe(II)

measured by a FerroZine assay. Fe(III) citrate cultures were inoculated 1:100 from a 0.5 OD₆₀₀ fumarate culture. A 0.1-ml sample of the Fe(III) citrate cultures was taken at regular intervals into 0.9 ml of 0.5 N HCl. This sample was used in a FerroZine assay to determine Fe(II) formed. FerroZine (Sigma; 2 g/liter in 0.1 M HEPES [pH 7]) forms a visible complex with Fe(II) and was measured at 625 nm. The amount of Fe(II) formed was compared to a standard curve with known concentrations of Fe(II)SO₄.

Stock Mn(IV) oxide was synthesized according to the method of Lovley and Phillips (17). Briefly, 3.16 g of KMnO₄/liter was dissolved in a 0.08 N NaOH solution. An equal volume of a 5.94-g/liter solution of MnCl₂·4H₂O was rapidly added to the KMnO₄ with vigorous stirring. The solution was allowed to settle for ~1 h at 4°C in the dark, after which the liquid was decanted, and the solid was centrifuged and washed in double-distilled H₂O (ddH₂O). A 1-ml aliquot of the mineral gel was allowed to dehydrate overnight at 37°C on a petri dish and weighed to determine the molarity of the mineral gel using the molecular weight of MnO₂ (86.9 g/mol). After the basal medium was cooled from the autoclave, the Mn(IV) oxide stock was added anaerobically to a final concentration of 20 mM in basal medium with 10 mM acetate. Mn(IV) oxide cultures were inoculated 1:100 from a 0.5 OD₆₀₀ fumarate culture. Samples were taken at regular intervals and dissolved 1:10 in acid with Fe(II) added. Because Mn(IV) is a strong electron acceptor, Fe(II) will reduce any Mn(IV) present under acidic conditions. A solution of 2 N HCl with 4 mM Fe(II)SO₄ reacted overnight and in the dark was sufficient for full reduction of 2 mM Mn(IV). A 1:5 dilution in 0.5 N HCl was performed prior to measuring the Fe(II) using the FerroZine assay described above. The amount of Mn(IV) reduction was calculated based on the amount of Fe(II) left in solution.

All inoculum cultures for growth using poised electrodes (0.24 V versus standard hydrogen electrode [SHE], VMP3 multichannel potentiostat; BioLogic) as the terminal electron acceptor were grown in acetate-

fumarate medium described above to an OD₆₀₀ of 0.5 from single colonies obtained from a fresh plate in an anaerobic glove box. Colonies were grown in 1 ml of medium and then transferred 1:10 into 10 ml of fresh acetate-fumarate medium. As this culture reached an OD₆₀₀ of 0.5, electrode bioreactor growth was initiated to achieve a density of 0.125 OD₆₀₀ in the bioreactor. Bioreactor medium was composed of 20 mM acetate basal medium with 2.9 g/liter NaCl added for osmotic balance to account for the lack of fumarate.

For *G. sulfurreducens*, kanamycin (200 µg/ml) was supplemented when needed unless otherwise stated. *Escherichia coli* K-12 strains were grown in Luria-Bertani medium (LB) supplemented with kanamycin (50 µg/ml) and 2,6-diaminopimelic acid (0.3 mM) when culturing *E. coli* strain BW29427 (this strain is also commonly referenced as WM3064).

Electrode bioreactor setup. Electrode bioreactors were assembled as previously described (18), with minor modifications. In all cases, 1500 grit wet/dry sandpaper (Ali Industries, Inc., Fairborn, OH) was used to polish the 3-cm² graphite working electrode. To remove residual graphite dust, polished electrodes were sonicated in ddH₂O with three water exchanges. Reactors were assembled using platinum wire counter electrodes and Calomel reference electrodes calibrated before each experiment against a master reference electrode. Assembled reactors were cleaned using alternating 1 N NaOH and 1 N HCl washes, with a final wash using ddH₂O to ensure a neutral pH. Reactors were then sterilized at 121°C for 20 min prior to use.

Growth-independent Fe(III) citrate reduction assay. Fe(III) citrate reduction was assayed in 10-ml anaerobic tubes or 96-well plates in real time with a buffered solution of Fe(III) citrate with FerroZine containing HEPES (50 mM), Fe(III) citrate (5 mM), sodium acetate (10 mM), NaCl (50 mM), KCl (5 mM), CaCl₂ (0.3 mM), MgSO₄ (0.8 mM), pH 6.8. For the 10-ml tube assay, hourly samples were diluted 1:10 into HCl (0.5 N) before performing a FerroZine (2 g/liter in 50 mM HEPES) assay using known concentrations of Fe(II)SO₄ as standards. In the real-time assay, FerroZine (2 g/liter) was added to the buffer containing Fe(III) citrate immediately before the addition of cells to the 96-well plates. The assay was initiated by the addition of a 10:1 volume of the solution to a fully grown fumarate culture and incubated inside an Omni-Lab (Vacuum Atmospheres Company; 100% N₂ atmosphere) monitoring the absorbance every 1 min at 625 nm in a SpectraMax M2 (Molecular Devices) over a 2-h period. Total cellular protein were determined by a bicinchoninic acid (Pierce) protein assay, and Fe(II)SO₄ standards in the real-time assay allowed all rates to be expressed as nmol of Fe(II) mg of total protein⁻¹ min⁻¹.

Conjugation of plasmids into *G. sulfurreducens*. All complementation and *sacB* suicide vectors were conjugated into *G. sulfurreducens* using *E. coli* donor strains S17-1 or BW29427. One milliliter of overnight LB culture of the donor strain with the plasmid was pelleted in a 1.6-ml centrifuge tube at 5,000 × g for 2 min, and the supernatant was discarded. Then, 1 ml of a growing 0.4 OD₆₀₀ *G. sulfurreducens* recipient culture was added to the centrifuge tube containing the *E. coli* donor strain inside the anaerobic workstation and pelleted at 2,000 × g for 3 min, and the supernatant was discarded. The cell mixture was resuspended in 40 µl of residual supernatant and incubated on sterile 0.22-µm-pore-size filter paper resting on an agar plate described above containing acetate-fumarate for 4 h in an anaerobic atmosphere before plating the mixture onto an acetate-fumarate plate with 200 µg of kanamycin/ml to select for *G. sulfurreducens* recipients.

Scarless gene deletion using *SacB*/sucrose counterselection. Deletion vectors were conjugated into *G. sulfurreducens* using donor mating strains S17-1 or BW29427. Integration of these plasmids into the chromosome was confirmed with flanking PCR primers. Integrants were plated onto acetate-fumarate agar plates containing 10% sucrose to select for a second recombination event to generate either the wild type (WT) or the deletion allele. Sucrose-resistant colonies were screened for kanamycin sensitivity on agar plates and sensitive colonies screened by PCR using flanking primers to confirm the deletion allele.

Plasmid construction. The primers and oligonucleotides used in the present study were ordered from IDT and are listed in Table 2. DNA was amplified using Phusion HSII polymerase (Thermo), digested with Fast-Digest restriction enzymes (Thermo), blunted with Fast DNA Repair kit (Thermo), and ligated with Fast-Link DNA ligase (Epicentre). All plasmids were extracted from cells using PureYield plasmid miniprep (Promega), and sequences were verified with Sanger sequencing in the University of Minnesota Genomics Center (UMGC).

pRK2-Geo1. The *acpP* (GSU1604) promoter region was generated by annealing and extending the primers *acpP1* and *acpP2* in a PCR. The product was digested with *AscI* and *NdeI* and ligated into the same sites in pRVMCS-2. The *acpP* promoter replaced the *vanR* gene and *vanA* promoter in pRVMCS-2 to generate pRK2-Geo1. The *acpP* promoter sequence cloned in pRK2-Geo1 includes the *acpP* RBS.

pRK2-Geo2 and pRK2-Geo2-lacZa. A fragment of the *bla* gene was excised from pRVMCS-2 using *Eam1150I* and *ScaI*, blunted, and religated to generate pRK2m1. The *nptI* gene was amplified with the primers *nptI1* and *nptI2* using pRVMCS-2 as a template and ligated into *BbsI*-digested and blunted pRK2m1 to generate pRK2m2. The *nptI* gene in pRK2m2 is in the reverse orientation as pRVMCS-2. Primer *oriV-rnnB-oriT* (gBlock) containing an *oriV* and *oriT* sequence with the *E. coli rnnB* transcription termination sequence was digested with *AccI* and *MscI* and ligated into the same sites in pRK2m2 to generate pRK2m3. The *acpP* (GSU1604) promoter region of pRK2-Geo1 was digested with *NotI* and *NheI* and ligated into the same sites in pRK2m3 to generate pRK2-Geo2. The fragment containing the *lacZa* in pSRK-Km was excised from pSKR-Km and ligated into the same site in pRK2-Geo2 to generate pRK2-Geo2-lacZa.

pRK2-Geo2i and pRK2-Geo2i-lacZa. Primer PGSU0800-*vanR*-*PacpP*-*vanA* (gBlock) containing the promoter regions of GSU0800 and a modified GSU1604 promoter region with *VanR* binding sites was digested with *NcoI* and *NdeI* and ligated into the same sites in pRVMCS-2 to generate pGVMCS-2. The modified promoter region in pGVMCS-2 was digested with *NotI* and *NheI* and ligated into the same sites in pRK2m3 to generate pRK2-Geo2i. The fragment containing the *lacZa* in pSRK-Km was excised from pSKR-Km and ligated into the same site in pRK2-Geo2i to generate pRK2-Geo2i-lacZa.

pRK2-Geo5. Primer *taclac* (gBlock) containing the *taclac* promoter region was digested with *AscI* and *NdeI* and ligated into the same sites in pRK2-Geo2 to generate pRK2-Geo5. The *taclac* promoter sequence with the RBS is identical to that in pCD341 (19).

pImcH vectors. GSU3259 (*imcH*) was amplified with the primers *imcH1* and *imcH2*, digested with *NdeI* and *XbaI* and ligated into the same sites in pSRK-Km to generate pImcH4. GSU3259 was subcloned from pImcH4 into pRK2-Geo2, pRK2-Geo2i, and pRK2-Geo5 using *NdeI* and *NheI* to generate pImcH15, pImcH16, and pImcH17, respectively.

Deletion vectors. The flanking regions (1,013 bp upstream and 1,078 bp downstream) of GSU0299 were amplified with the primer sets 0299-1F/0299-1R and 0299-2F/0299-2R using genomic DNA as the template. The flanking regions of GSU0299 were joined in a second round of PCR, digested with *BamHI* and *SpeI*, and then ligated into the same sites in pSMV3 to generate pDGSU0299. The flanking regions (914 bp upstream and 1,072 bp downstream) of *imcH* were amplified with the primer sets *imcH-1F/imcH-1R* and *imcH-2F/imcH-2R* using genomic DNA as the template. The flanking regions of *imcH* were joined in a second round of PCR, digested with *BamHI* and *SpeI*, and then ligated into the same sites in pSMV3 to generate pDImcH1. A second deletion plasmid of *imcH* was constructed in pK18mobsacB using the primer sets *imcH-K1F/imcH-K1R* and *imcH-K2F/imcH-K2R*. The fragments were joined as described above, digested with *HindIII* and *BamHI*, and then ligated into pK18mobsacB to generate pDImcH2.

Sequencing. Plasmids pRK2-Geo2, pRK2-Geo2i, and pRK2-Geo5 were sequenced by including plasmids in unrelated *G. sulfurreducens* genomic DNA sequencing projects using Illumina MiSeq 2×250 single lane at the UMG. Debarcoded sequences were assembled using SPAdes (version 3.5; Algorithmic Biology Lab/St. Petersburg Academic University

TABLE 2 Primers used in this study

| Function and primer | Sequence (5'-3') |
|--------------------------------------|--|
| Complementation vectors | |
| acpP1 | ACACGGCGCGCCTATCTTTTGAATTTAGGCGTTTCGTGGTATGTAGCTAGAAACATTAC |
| acpP2 | CTGTCATATGGCTTGTTCACCTCCGTTTGGTTTGGTCTTCGGGTAATGTTTCTAGCTAC |
| nptI1 | GAGACGTTGATCGGCACGTAAG |
| nptI2 | GGTGTGCTGACTCATAACCAG |
| oriV-rrnB-oriT | TAATACGACTCACTATAGGGTGGCCAGCTCCACGTCGCCGCGCAAATCGAGCCTGCCCTCATCTGTCAACGC CGCGCCGGGTGAGTCGGCCCCTCAAGTGTCAACGTCGCCCCCTCATCTGTCAAGTGGCCAAAGTTTCC GCGTGGTATCCACAACGCCGGCGGCCCTACATGGCTCTGCCGACAAACAACAGATAAAACGAAAGGCC CAGTCTTTCGACTGAGCCTTTCGTTTATTTGGATCCACTAGTTCTAGAGCGGCCATCGACGGATCTTTT CCGCTGCATAACCCTGCTTCGGGGTCATTATAGCGATTTTTTCGGTATATCCATCCTTTTTTCGCACGA TATACAGGATTTTGCCAAAGGGTTCGTGTAGACCCGCTGAGCAATAACTAGC |
| PGSU0800-vanR-PacpP-vanA | TAATACGACTCACTATAGGGCCATGGCAGCAATACGAGTTTTTTCACGTTTCGGCACCTCTCCTTAAATGAATT TAACTGCATGGAACAACAATTTGCCAACACCGAACGCGAATTATTGCAGAAAGGTGACAGTGCCTCAAGT AATGCTGGACTCTAGCCGACCGACTGAGACGCTCAACAAGCGTTCAATTGGATCCAATCTTGAAATTTA GGCGTTTCGTGGTATGTATTGGATCCAATTTACCCGAAGACTCAAACCAACGGAGGTGAACAAGCCATA TGCCGCTGAGCAATAACTAGC |
| taclac | TAATACGACTCACTATAGGGGGCGCGCCTTGACAATTAATCATCGGCTCGTATAATGTGTGGAATTGTGAGCGG ATAACAATTTACACAGGAACTAGGCACCCAGGCTTTACACTTTATGCTTCCGGCTCGTATGTTGTGT GGAATTGTGAGCGGATAACAATTTACACAGGAAACACATATGCCGCTGAGCAATAACTAGC |
| Deletion vectors | |
| 0299-1F | CGCGGATCCAGCTCACGTCATGCCGTCAAG |
| 0299-1R | GCGGTGAAGCGGTCGAGGAAGGTGTGACCAGAAGGGGGATG |
| 0299-2F | CATCCCCTTCTGGTCAACACCTTCTCGACCGCTTCAACCGC |
| 0299-2R | CGACTAGTGCCAGGTCTTGTGATATCGC |
| imcH-1F | CGCGGATCCGGATCTCATCACCCCGTATCCGA |
| imcH-1R | GGAGGAGATGTATGACATTGCGCAAGCACTGACACGGCCTGCAG |
| imcH-2F | CTGCAGGCCGTGTCAGTGCTTGGCAATGCATACATCTCCTCC |
| imcH-2R | CGACTAGTGAAGATGCAGCAGTCGATGCC |
| imcH-K1F | GCTA AAGCTT CAATTCGTAAGTCTCGGCACCG |
| imcH-K1R | GGAGGAGATGTATGACATTGCGCAAGCACTGACACGGCCTGCAG |
| imcH-K2F | CTGCAGGCCGTGTCAGTGCTTGGCAATGCATACATCTCCTCC |
| imcH-K1R | GCTAGGATCC GGCCAGTGCTGATCCACGATT |
| Confirmation of gene deletion | |
| 0299-up-F | TTACGTGCTCAGCGCATTCCGG |
| 0299-down-R | GTGTCTCACGAGGGAGCAGA |
| imcH-up-F | CTGCCATCAGCTCTGTTACC |
| imcH-down-R | CCTTACTGTCTGGCACGG |
| imcH vector | |
| imcH1 | ACGCCATATGACATTGCGCAAA ACCGCAG |
| imcH2 | CGCTTAGATTGCTGCTGCAGCCGTGTCAG |

of the Russian Academy of Sciences [<http://bioinf.spbau.ru/spades>] and a reference *G. sulfurreducens* genome as a trusted contig. MUMmer (version 3.23 [<http://mummer.sourceforge.net>]) was used to isolate the plasmid sequences remaining in the unmatched SPAdes scaffolds. Plasmid circularity was confirmed via dot plot, and self-overlapping ends were manually trimmed. Sequences were reconfirmed by mapping reads to the assembled contigs using breseq (version 0.24rc6; Barrick Lab/University of Texas at Austin [<http://barricklab.org/wiki/bin/view/Lab/ToolsBacterialGenomeResequencing>]) (20).

To accurately design primers for mutants and verify the outcome of deletion experiments, a complete genome of our laboratory strain was assembled. Genomic DNA (5 µg) was used to generate a 20-kb insert library for PacBio long-read sequencing, and the library was size selected to >7 kb with the BluePippin electrophoresis system (Sage Science). *De novo* assembly was performed with HGAP v3 (21) in SMRT Analysis v2.2 on filtered subreads >12 kb (minimum quality 0.8) to provide 100× coverage, polished using the entire read set (~190×) to >99.999% consensus concordance (QV 50) with three successive passes through Quiver

(21). A total of 123 remaining indels were removed by mapping 85× coverage of 2×250-bp Illumina reads using Pilon v1.10 (22).

ΔGSU0299 genomic DNA (0.3 µg) was submitted to UMGC for a 2×250-bp paired-end MiSeq, demultiplexed to 2 million reads and mapped against our *G. sulfurreducens* genome using breseq with default parameters.

NCBI accession numbers. Complete read files for our laboratory strain, the ΔGSU0299 strain, and the plasmids have been deposited in the NCBI Sequence Read Archive database under accession numbers [SRX101230](https://www.ncbi.nlm.nih.gov/sra/SRX101230), [SRX1101232](https://www.ncbi.nlm.nih.gov/sra/SRX1101232), and [SRX1101235](https://www.ncbi.nlm.nih.gov/sra/SRX1101235), respectively. Plasmid sequences for pRK2-Geo2, pRK2-Geo2i, and pRK2-Geo5 have been deposited in the NCBI GenBank database with accession numbers [KT339318](https://www.ncbi.nlm.nih.gov/nuccore/KT339318), [KT339319](https://www.ncbi.nlm.nih.gov/nuccore/KT339319), and [KT339320](https://www.ncbi.nlm.nih.gov/nuccore/KT339320), respectively.

RESULTS

Generating a markerless deletion of GSU0299 to enable motility. FrgM is a regulator of flagellar synthesis (6), but in the *G.*

sulfurreducens genome, the bona fide *frgM* gene is interrupted by a transposase (GSU0299), inactivating motility. We selected GSU0299 as a target for a SacB/sucrose counterselection strategy as a proof-of-concept, as this required a precise scarless in-frame deletion for gain of function.

E. coli conjugation donor strains are able to transfer plasmids containing mobilization genes (*mob*) and an origin of transfer (*oriT*) into *G. sulfurreducens* (5). In preliminary screening, the S17-1 *E. coli* donor strain was more efficient in transferring *mob* vectors into *G. sulfurreducens* compared to the previously reported *E. coli* donor strain BW29427. The *sacB* and *kanR* encoding vectors pSMV3 and pK18mobsacB, which are unable to replicate in *G. sulfurreducens*, were engineered to contain homologous regions flanking GSU0299. These plasmids integrated into either flanking region of GSU0299 when transconjugants were plated on medium containing kanamycin. Strains in which removal of GSU0299 occurred via a second recombination event were selected by growing transconjugants on 10% sucrose medium (Fig. 1A). The activity of SacB in the presence of sucrose was inhibitory to *G. sulfurreducens* (23), and sucrose-resistant colonies were screened for kanamycin sensitivity, indicating loss of the plasmid. Approximately 20% of isolates were still resistant to kanamycin after sucrose selection, likely due to inactivation of *sacB*, while PCR screening and sequencing revealed 50% of the kanamycin-sensitive isolates had the desired mutation (Fig. 1B).

The resulting Δ GSU0299 strain spread from sites of inoculation in motility medium containing 0.4% agar (Fig. 1D). Full genome resequencing confirmed the Δ GSU0299 deletion was in-frame and was the only mutation compared to the parent strain (Fig. 1C). Ten times more *G. sulfurreducens* transconjugants were isolated using the higher-copy-number *sacB* plasmid pK18mobsacB compared to pSMV3. A similar approach was then used with pK18mobsacB to delete *imcH*, an inner membrane cytochrome required for reduction of high redox potential electron acceptors such as Fe(III) citrate, Mn(IV) oxides, and electrodes poised at potentials > -0.1 V versus SHE (7). The subsequent $\Delta imcH$ strain was used to study the different vectors and promoters useful in complementation and induced expression.

Development of stable replicating expression vectors for *G. sulfurreducens*. Two broad-host-range backbones are routinely used for complementation in *G. sulfurreducens*. We compared the effects of pSRK (pBBR1 origin) and pRVMCS-2 (RK2 origin, IncP) on *G. sulfurreducens* growth in the presence of kanamycin (24, 25). Cells carrying the pBBR1 plasmid had a longer doubling time ($\sim 33\%$) and demonstrated measurable lag compared to WT when fumarate was the terminal electron acceptor (Fig. 2A). The RK2 plasmid only slowed doubling times by $\sim 15\%$ in the presence of kanamycin and showed no lag. The copy number was higher for pBBR1, at ~ 50 copies per cell versus ~ 5 copies per cell for RK2. This increased burden may contribute to the known instability of pBBR plasmids in *G. sulfurreducens* cells (9). Eighty-five percent of *G. sulfurreducens* cells retained the RK2 vector after over 15 generations in liquid acetate-fumarate medium in the absence of kanamycin selection by plating dilutions after liquid growth on plates containing kanamycin, whereas the pBBR1 vector was rapidly cured, similar to previous observations (9). Therefore, we selected RK2-based plasmids as the basis for a new expression system.

To generate constitutive expression vectors, we first replaced the *vanA* promoter, *vanR* and *bla* genes in the *Caulobacter crescent-*

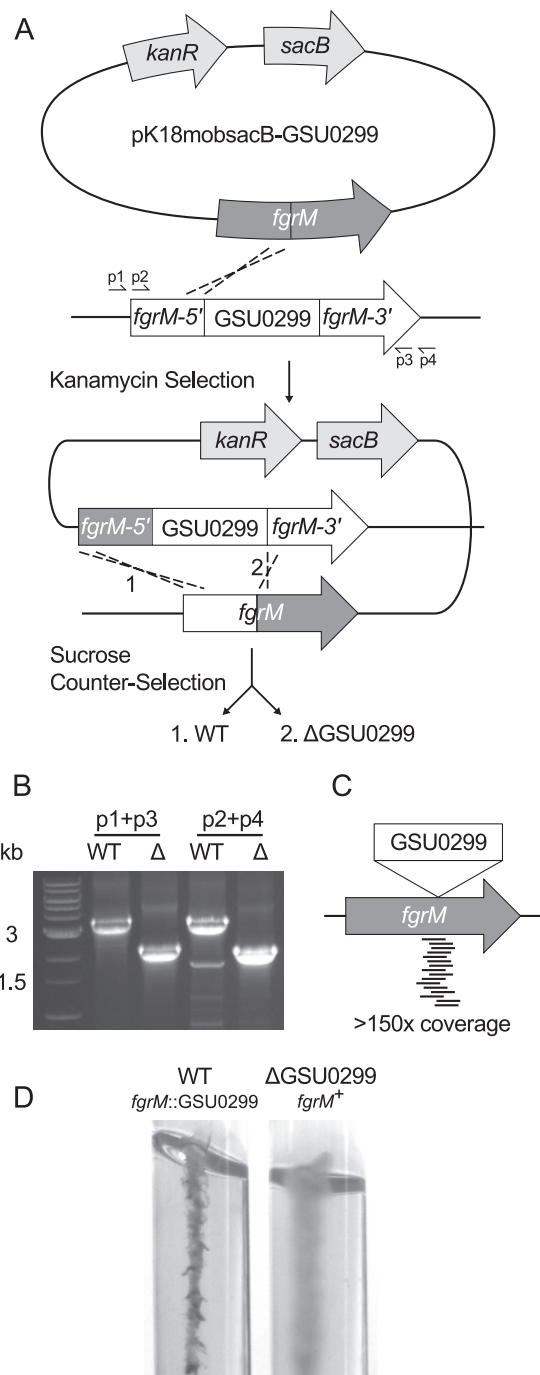


FIG 1 Markerless deletion of GSU0299 from the *G. sulfurreducens* genome. (A) Flanking sequences of the GSU0299 transposon in the *sacB* vector pK18mobsacB integrate in this example upstream of GSU0299 in the presence of kanamycin. Cells plated on sucrose select for a second recombination event that can either generate the WT or the deletion allele. (B) Primers p1 to p4 depicted in panel A screen for deletion of GSU0299. (C) Full genome sequencing found $150\times$ coverage of reads spanning the deletion junction in *frgM*, verifying the transposon was removed. No reads spanned the WT junction, and no other mutations were found in the Δ GSU0299 genome. (D) The resulting Δ GSU0299, *frgM*⁺ cells grew from the point of inoculation in 0.4% agarose, indicating motility compared to the nonmotile WT.

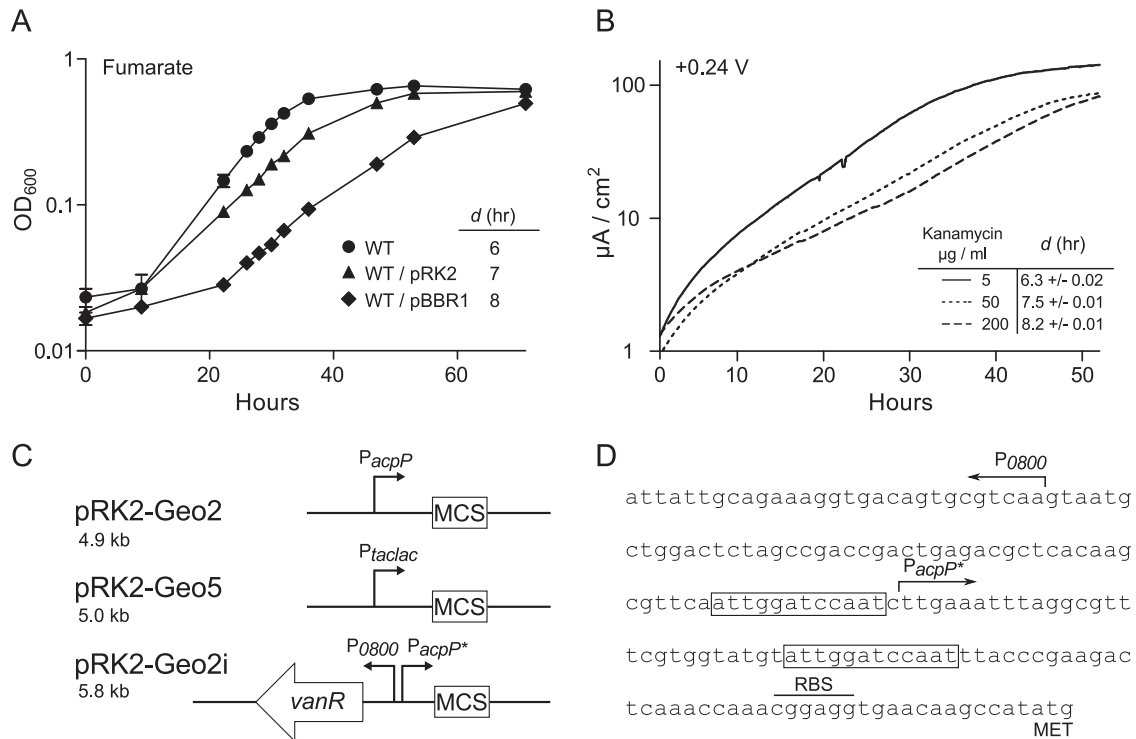


FIG 2 Slower doubling times with pBBR1 and kanamycin inhibition of biofilm growth on electrodes (A) *G. sulfurreducens* cells had a longer doubling time (*d*) in fumarate medium when carrying the high copy number plasmid pBBR1 (pSRK-Km) compared to WT and WT carrying pRK2 (pRVMCS-2; ± the standard deviations [SD]; *n* = 3 for each condition, 200 μg of kanamycin/ml added to plasmid-containing cultures). (B) WT *G. sulfurreducens* carrying pRK2-Geo2i reached a lower current density on electrodes poised at 0.24 V versus SHE at 50 h and had a longer doubling time (*d*) in the presence of both low (50 μg/ml) and normal (200 μg/ml) levels of kanamycin. (Representative curve from *n* = 6 for 5 μg/ml; *n* = 7 for 50 μg/ml, and *n* = 2 for 200 μg/ml kanamycin). (C) Promoter regions designed for vectors described in the present study. The multiple cloning site (MCS) contains the following unique restriction sites: NdeI, EcoRI, KpnI, PmlI, DraIII, SacI, AflII, BglII, SnaBI, AgeI, NheI, and PstI. (D) Sequence of the pRK2-Geo2i-inducible promoter. The GSU0800 promoter controls *vanR* expression. VanR binding sites on the modified *acpP* promoter are highlighted by boxes, and the ribosome binding site (RBS) and start codon (MET) are indicated.

tus plasmid pRVMCS-2 with the *G. sulfurreducens acpP* (GSU1064) promoter or the *E. coli* based *taclac* promoter to generate pRK2-Geo2 and pRK2-Geo5, respectively (Fig. 2C). Both *acpP* transcripts and the AcpP protein are highly abundant across multiple conditions, and its transcription is only regulated by the housekeeping sigma factor RpoD (26, 27). The native *acpP* promoter was modified to include palindromic VanR binding sites, and expression of *vanR* was driven by another constitutive RpoD-dependent promoter (GSU0800), creating the vanillate-inducible vector pRK2-Geo2i (Fig. 2D) (25).

In preliminary work, cloning *imcH* under the control of the *C. crescentus vanA* promoter in pRVMCS-2 did not complement growth of the $\Delta imcH$ strain in Fe(III) citrate in the presence or absence of vanillate, suggesting that *Geobacter* did not recognize the *Caulobacter vanA* or *vanR* promoters. When the constitutive *G. sulfurreducens acpP* (GSU1064) promoter was used to express *imcH* in the pRK-Geo2 backbone (pImcH15), this construct fully complemented growth of the $\Delta imcH$ strain (Fig. 3A). When *imcH* was cloned into the inducible pRK-Geo2i vector (pImcH16), reduction of Fe(III) by the $\Delta imcH$ strain was triggered even when vanillate was added 24 h after inoculation (Fig. 3A). To further confirm the pRK2-Geo2i-inducible vector could be used in the study of insoluble electron acceptors, we demonstrated that Mn(IV) reduction only occurred in $\Delta imcH$ /pImcH16 cultures when vanillate was added (Fig. 3B) (7). In addition, both the con-

stitutive *acpP* and the modified vanillate-inducible promoters in pRK2-Geo2 and pRK2-Geo2i were recognized by *E. coli*. When the *lacZ* fragment was cloned downstream of *acpP*, blue colonies were produced on LB X-Gal (5-bromo-4-chloro-3-indolyl- β -D-galactopyranoside) plates. In the pRK2-Geo2i-*lacZ* construct, *E. coli* colonies turned blue only in the presence of vanillate.

While studying growth of kanamycin cassette insertional mutants on electrodes, we noticed a correlation between low inoculum levels and higher growth rates and hypothesized that this was due to reduced carryover of antibiotics. To test this effect further, WT cells containing pRK2-Geo2i were precultured in fumarate medium, and after dilution into a poised electrode bioreactor the concentration of antibiotic carried over was 5 μg/ml. Additional kanamycin was then added to bioreactors to concentrations typically used for mutant and plasmid selection (200 μg/ml), as well as a concentration representing only 25% of this level. Even low concentrations of antibiotic significantly slowed growth and decreased the final current density of the biofilms (Fig. 2B). These experiments confirmed that, even with an appropriate resistance gene present, sublethal levels of kanamycin alter the outcome of experiments. For subsequent experiments, all preculturing and inoculation was done to achieve <5 μg of kanamycin/ml in electrode reactors, since these plasmids are maintained for multiple generations without antibiotic selection.

Compared to planktonic growth with Fe(III) citrate, induction

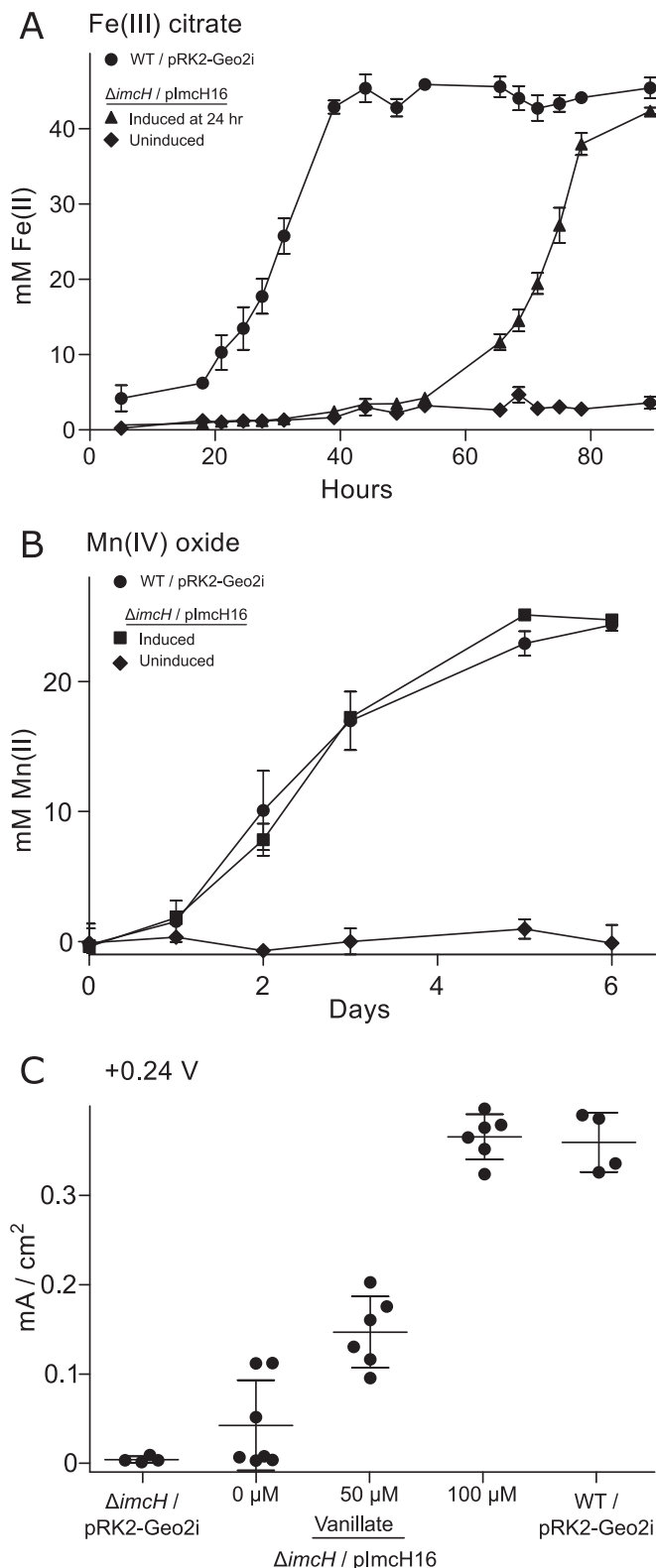


FIG 3 Vanillate induction under Fe(III) citrate, Mn(IV) oxide, and poised electrode growth conditions. (A) Growth using Fe(III) citrate as the terminal electron acceptor in WT carrying the empty vector pRK2-Geo2i (●) and $\Delta imcH$ strain carrying pImcH16 ($imcH^+$ in pRK2-Geo2i). $\Delta imcH/plmCH16$ cells were induced with 50 μM vanillate at 24 h (▲) or left uninduced (◆). (Results are indicated as \pm the SD; $n = 3$ for each condition). (B) Mn(IV)

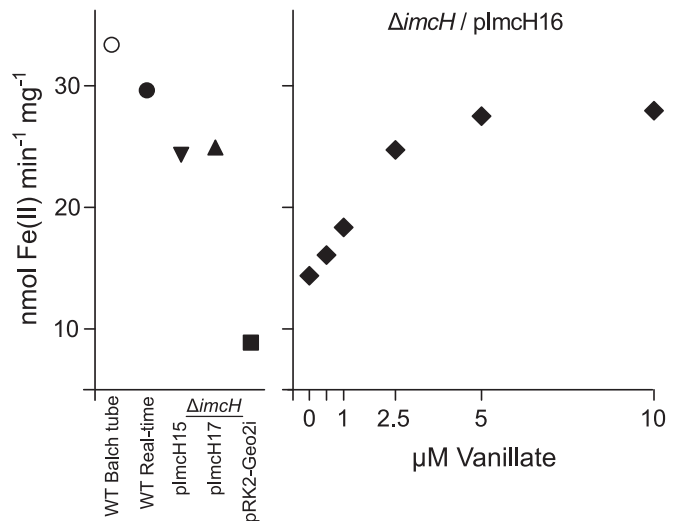


FIG 4 Real-time Fe(III) citrate reduction assay. Fe(III) citrate reduction by WT in 10-ml Balch tubes (○) compared to WT in the real-time 96-well assay (●). The levels of complementation of the $\Delta imcH$ strain by $imcH$ cloned under the native constitutive promoter $acpP$ in pImcH15 (▼), the $tacIac$ promoter in pImcH17 (▲), and the empty vanillate-inducible vector pRK2-Geo2i (■) were compared. Increasing concentrations of vanillate inducer in the culture used to grow cells increased Fe(III) citrate reduction rates in the $\Delta imcH$ strain carrying the inducible pImcH16 (◆). (Results are indicated as \pm the SD; $n = 3$ for each condition). The rates of Fe(III) citrate reduction were normalized to the amount of cell protein.

in biofilms may respond differently. To determine whether the vanillate system could be used to restore wild-type rates of electron transfer to electrodes, $\Delta imcH$ cells carrying the inducible plasmid pImcH16 were inoculated into bioreactors poised at +0.24 V versus SHE. The addition of vanillate after inoculation immediately triggered growth. However, a higher concentration than what was used for Fe(III) citrate was needed to reach WT growth rates and biofilm current densities (Fig. 3C).

High-throughput Fe(III) citrate reduction assay. A spectrophotometric 96-well plate assay was developed to quickly compare rates of Fe(III) citrate reduction and screen the array of plasmids, promoters, and mutants created in this study (28). This real-time assay measures Fe(III) reduction independent of growth due to a lack of phosphate, nitrogen, mineral, and carbon dioxide sources in the reaction. The assay is initiated by the addition of cells directly in a FerroZine-containing, Fe(III) citrate buffer. Previously, our growth independent Fe(III) citrate reduction assay was performed in 10-ml Balch tubes for >4 h, requiring samples to be taken by syringe per time point and analyzed via mixing with FerroZine reagent. In a direct comparison of these methods, rates of Fe(III) citrate reduction per mg of protein by WT cells in the 96-well plate method were similar to rates measured using the longer 10-ml Balch tube assay (Fig. 4).

oxide reduction by WT *G. sulfurreducens* carrying pRK2-Geo2i (●) compared to $\Delta imcH$ carrying pImcH16 with (■) and without (◆) induction by 50 μM vanillate. (Results are indicated as \pm the SD; $n = 3$ for each condition). (C) Current density on electrodes poised at 0.24 V versus SHE at 80 h, comparing WT carrying empty pRK2-Geo2i to $\Delta imcH$ carrying pRK2-Geo2i, and $\Delta imcH$ carrying the vanillate-inducible pImcH16 with 50 and 100 μM vanillate added at the time of inoculation. (Results are indicated as \pm the SD, each point = one independent reactor; $n = 27$ reactors in total).

To demonstrate the utility of the real-time assay, complementation of the $\Delta imcH$ strain by two different complementation vectors, pImcH15 (pRK2-Geo2), and pImcH17 (pRK2-Geo5), along with the inducible pImcH16 (pRK2-Geo2i) was compared. Both pImcH15 and pImcH17 restored near WT Fe(III) citrate reduction rates, and increasing rates of Fe(III) reduction were achieved by increasing vanillate concentrations from 0 to 10 μM (Fig. 4). The concentrations required to elicit full induction in the *Geobacter* VanR-inducible system were similar to those previously reported in *Caulobacter* and *Myxococcus*, with the response range in the low-micromolar levels (25, 29). A background rate of Fe(III) reduction in the absence of vanillate was detectable in the nongrowth assay, suggesting a low level of *imcH* expression from pImcH16 or background activity due to other inner membrane cytochromes. Since growth on Fe(III) citrate was not detected in the same strain in the absence of vanillate (Fig. 3A), this demonstrated the increased sensitivity of the nongrowth real-time Fe(III) citrate reduction assay in detecting residual electron transfer activity in mutants.

DISCUSSION

Precise removal and insertion of DNA into the *G. sulfurreducens* chromosome enabled by the SacB/sucrose counter selection strategy allows for construction of multigene deletion and insertion mutants without the effects of polarity or undesired changes in the chromosome. While weeks of anaerobic manipulation are required to generate a mutation using the two-step method, the resulting strain is not burdened by expression of antibiotic resistance cassettes, increasing the availability of markers for maintenance of expression plasmids. Researchers should take caution in the use of antibiotics, since we show the aminoglycoside kanamycin is inhibitory even when cells are expressing a resistance gene. Gentamicin, another aminoglycoside, showed similar inhibitory effects on cell growth even when respiring to a soluble electron acceptor in our preliminary studies, and therefore was not considered as we developed plasmids for this work. This underscores the need for proper empty-vector controls conducted under similar conditions in genetic studies.

Ectopic expression in *G. sulfurreducens* previously relied on broad-host-range plasmids of unknown copy number from promoters with unknown strengths, which could partly explain the incomplete complementation of mutations in *Geobacter* (5, 7, 13). By using a more stable, low-copy-number plasmid and modifying a constitutively expressed promoter (*acpP*), we have the ability to control gene expression by the addition of a small, nontoxic, membrane permeable molecule. Since we developed these vectors using a crucial respiratory cytochrome as the benchmark for full complementation, analyses of other physiologically relevant genes involved in metal respiration should be possible. For more complex genetic circuitry or multigene expression analysis, future work will need to engineer additional inducible expression systems with other membrane permeable compounds such as benzoate or short-chain fatty acids.

To accelerate the development of expression vectors and analyze the complex electron transfer pathway of *Geobacter*, a sensitive kinetic assay is necessary. A real-time Fe(III) citrate assay proved to be faster and use less reagent than the discontinuous assay. This nongrowth assay appears to detect residual rates of electron transfer in $\Delta imcH$ mutants that were too slow to support growth and that were not easily detectable in the traditional assay.

Part of this increased sensitivity could come from the presence of the Fe(II)-trapping reagents poisoning the Fe(III)/Fe(II) ratio consistently high, keeping electron transfer favorable. This sensitivity and consistency will be useful in the search for secondary or overlapping electron transfer mechanisms.

The genetic tools presented here will aid future genetic manipulation of *G. sulfurreducens*, and minimize confounding factors such as antibiotic inhibition or stability of vectors. This system offers a much needed ability to directly manipulate gene expression levels in *Geobacter* and provides an example of how *Geobacter* can be engineered to produce electrical current upon sensing an external signal (30). This combination of genetic precision and transcriptional control is a crucial part of any biosensor or biodevice based on extracellular electron transfer.

ACKNOWLEDGMENTS

We thank P. Mera in the L. Shapiro laboratory, M. Spero in the T. Donohue laboratory, and J. Will in the J. Escalante-Semerena laboratory for providing strains and plasmids used in this work.

This study was supported by grant N000141210308 from the Office of Naval Research and grant DE-SC0006868 from the Department of Energy (Biological and Environmental Research).

REFERENCES

- Brophy JAN, Voigt CA. 2014. Principles of genetic circuit design. *Nat Methods* 11:508–520. <http://dx.doi.org/10.1038/nmeth.2926>.
- Leigh JA, Albers S-V, Atomi H, Allers T. 2011. Model organisms for genetics in the domain Archaea: methanogens, halophiles, *Thermococcales* and *Sulfolobales*. *FEMS Microbiol Rev* 35:577–608. <http://dx.doi.org/10.1111/j.1574-6976.2011.00265.x>.
- Woodson JD, Escalante-Semerena JC. 2004. CbiZ, an amidohydrolase enzyme required for salvaging the coenzyme B₁₂ precursor cobinamide in archaea. *Proc Natl Acad Sci U S A* 101:3591–3596. <http://dx.doi.org/10.1073/pnas.0305939101>.
- McMahon MD, Guan C, Handelsman J, Thomas MG. 2012. Metagenomic analysis of *Streptomyces lividans* reveals host-dependent functional expression. *Appl Environ Microbiol* 78:3622–3629. <http://dx.doi.org/10.1128/AEM.00044-12>.
- Rollefson JB, Stephen CS, Tien M, Bond DR. 2011. Identification of an extracellular polysaccharide network essential for cytochrome anchoring and biofilm formation in *Geobacter sulfurreducens*. *J Bacteriol* 193:1023–1033. <http://dx.doi.org/10.1128/JB.01092-10>.
- Ueki T, Leang C, Inoue K, Lovley DR. 2012. Identification of multicomponent histidine-aspartate phosphorelay system controlling flagellar and motility gene expression in *Geobacter* species. *J Biol Chem* 287:10958–10966. <http://dx.doi.org/10.1074/jbc.M112.345041>.
- Levar CE, Chan CH, Mehta-Kolte MG, Bond DR. 2014. An inner membrane cytochrome required only for reduction of high redox potential extracellular electron acceptors. *mBio* 5:e02034. <http://dx.doi.org/10.1128/mBio.02034-14>.
- Mehta T, Coppi MV, Childers SE, Lovley DR. 2005. Outer membrane *c*-type cytochromes required for Fe(III) and Mn(IV) oxide reduction in *Geobacter sulfurreducens*. *Appl Environ Microbiol* 71:8634–8641. <http://dx.doi.org/10.1128/AEM.71.12.8634-8641.2005>.
- Coppi MV, Leang C, Sandler SJ, Lovley DR. 2001. Development of a genetic system for *Geobacter sulfurreducens*. *Appl Environ Microbiol* 67:3180–3187. <http://dx.doi.org/10.1128/AEM.67.7.3180-3187.2001>.
- Voordeckers JW, Kim B-C, Izallalen M, Lovley DR. 2010. Role of *Geobacter sulfurreducens* outer surface *c*-type cytochromes in reduction of soil humic acid and anthraquinone-2,6-disulfonate. *Appl Environ Microbiol* 76:2371–2375. <http://dx.doi.org/10.1128/AEM.02250-09>.
- Rollefson JB, Levar CE, Bond DR. 2009. Identification of genes involved in biofilm formation and respiration via mini-Himar transposon mutagenesis of *Geobacter sulfurreducens*. *J Bacteriol* 191:4207–4217. <http://dx.doi.org/10.1128/JB.00057-09>.
- Mahadevan R, Bond DR, Butler JE, Esteve-Nuñez A, Coppi MV, Palsson BO, Schilling CH, Lovley DR. 2006. Characterization of metabolism in the Fe(III)-reducing organism *Geobacter sulfurreducens* by con-

- straint-based modeling. *Appl Environ Microbiol* 72:1558–1568. <http://dx.doi.org/10.1128/AEM.72.2.1558-1568.2006>.
13. Leang C, Coppi MV, Lovley DR. 2003. OmcB, a *c*-type polyheme cytochrome, involved in Fe(III) reduction in *Geobacter sulfurreducens*. *J Bacteriol* 185:2096–2103. <http://dx.doi.org/10.1128/JB.185.7.2096-2103.2003>.
 14. Tremblay P-L, Aklujkar M, Leang C, Nevin KP, Lovley D. 2012. A genetic system for *Geobacter metallireducens*: role of the flagellin and pilin in the reduction of Fe(III) oxide. *Environ Microbiol Rep* 4:82–88. <http://dx.doi.org/10.1111/j.1758-2229.2011.00305.x>.
 15. Summers ZM, Ueki T, Ismail W, Haveman SA, Lovley DR. 2012. Laboratory evolution of *Geobacter sulfurreducens* for enhanced growth on lactate via a single-base-pair substitution in a transcriptional regulator. *ISME J* 6:975–983. <http://dx.doi.org/10.1038/ismej.2011.166>.
 16. Marx CJ, Lidstrom ME. 2002. Broad-host-range *cre-lox* system for antibiotic marker recycling in Gram-negative bacteria. *Biotechniques* 33:1062–1067.
 17. Lovley DR, Phillips EJ. 1986. Organic matter mineralization with reduction of ferric iron in anaerobic sediments. *Appl Environ Microbiol* 51:683–689.
 18. Marsili E, Rollefson JB, Baron DB, Hozalski RM, Bond DR. 2008. Microbial biofilm voltammetry: direct electrochemical characterization of catalytic electrode-attached biofilms. *Appl Environ Microbiol* 74:7329–7337. <http://dx.doi.org/10.1128/AEM.00177-08>.
 19. Dehio M, Knorre A, Lanz C, Dehio C. 1998. Construction of versatile high-level expression vectors for *Bartonella henselae* and the use of green fluorescent protein as a new expression marker. *Gene* 215:223–229. [http://dx.doi.org/10.1016/S0378-1119\(98\)00319-9](http://dx.doi.org/10.1016/S0378-1119(98)00319-9).
 20. Barrick JE, Colburn G, Deatherage DE, Traverse CC, Strand MD, Borges JJ, Knoester DB, Reba A, Meyer AG. 2014. Identifying structural variation in haploid microbial genomes from short-read resequencing data using *breseq*. *BMC Genomics* 15:1039. <http://dx.doi.org/10.1186/1471-2164-15-1039>.
 21. Chin C-S, Alexander DH, Marks P, Klammer AA, Drake J, Heiner C, Clum A, Copeland A, Huddleston J, Eichler EE, Turner SW, Korlach J. 2013. Nonhybrid, finished microbial genome assemblies from long-read SMRT sequencing data. *Nat Methods* 10:563–569. <http://dx.doi.org/10.1038/nmeth.2474>.
 22. Walker BJ, Abeel T, Shea T, Priest M, Abouelliel A, Sakthikumar S, Cuomo CA, Zeng Q, Wortman J, Young SK, Earl AM. 2014. Pilon: an integrated tool for comprehensive microbial variant detection and genome assembly improvement. *PLoS One* 9:e112963. <http://dx.doi.org/10.1371/journal.pone.0112963>.
 23. Gay P, Le Coq D, Steinmetz M, Berkelman T, Kado CI. 1985. Positive selection procedure for entrapment of insertion sequence elements in gram-negative bacteria. *J Bacteriol* 164:918–921.
 24. Khan SR, Gaines J, Roop RM, Farrand SK. 2008. Broad-host-range expression vectors with tightly regulated promoters and their use to examine the influence of TraR and TraM expression on Ti plasmid quorum sensing. *Appl Environ Microbiol* 74:5053–5062. <http://dx.doi.org/10.1128/AEM.01098-08>.
 25. Thanbichler M, Iniesta AA, Shapiro L. 2007. A comprehensive set of plasmids for vanillate- and xylose-inducible gene expression in *Caulobacter crescentus*. *Nucleic Acids Res* 35:e137. <http://dx.doi.org/10.1093/nar/gkm818>.
 26. Ding Y-HR, Hixson KK, Giometti CS, Stanley A, Esteve-Núñez A, Khare T, Tollaksen SL, Zhu W, Adkins JN, Lipton MS, Smith RD, Mester T, Lovley DR. 2006. The proteome of dissimilatory metal-reducing microorganism *Geobacter sulfurreducens* under various growth conditions. *Biochim Biophys Acta* 1764:1198–1206. <http://dx.doi.org/10.1016/j.bbapap.2006.04.017>.
 27. Qiu Y, Nagarajan H, Embree M, Shieu W, Abate E, Juárez K, Cho B-K, Elkins JG, Nevin KP, Barrett CL, Lovley DR, Palsson BO, Zengler K. 2013. Characterizing the interplay between multiple levels of organization within bacterial sigma factor regulatory networks. *Nat Commun* 4:1755. <http://dx.doi.org/10.1038/ncomms2743>.
 28. Childers SE, Lovley DR. 2001. Differences in Fe(III) reduction in the hyperthermophilic archaeon, *Pyrobaculum islandicum*, versus mesophilic Fe(III)-reducing bacteria. *FEMS Microbiol Lett* 195:253–258. <http://dx.doi.org/10.1111/j.1574-6968.2001.tb10529.x>.
 29. Iniesta AA, García-Heras F, Abellón-Ruiz J, Gallego-García A, Elías-Arnanz M. 2012. Two systems for conditional gene expression in *Myxococcus xanthus* inducible by isopropyl- β -D-thiogalactopyranoside or vanillate. *J Bacteriol* 194:5875–5885. <http://dx.doi.org/10.1128/JB.01110-12>.
 30. Golitsch F, Bücking C, Gescher J. 2013. Proof of principle for an engineered microbial biosensor based on *Shewanella oneidensis* outer membrane protein complexes. *Biosens Bioelectron* 47:285–291. <http://dx.doi.org/10.1016/j.bios.2013.03.010>.
 31. Simon R, Priefer U, Pühler A. 1983. A broad host range mobilization system for *in vivo* genetic engineering: transposon mutagenesis in Gram-negative bacteria. *Nat Biotechnol* 1:784–791. <http://dx.doi.org/10.1038/nbt1183-784>.
 32. Saltikov CW, Cifuentes A, Venkateswaran K, Newman DK. 2003. The *ars* detoxification system is advantageous but not required for As(V) respiration by the genetically tractable *Shewanella* species strain ANA-3. *Appl Environ Microbiol* 69:2800–2809. <http://dx.doi.org/10.1128/AEM.69.5.2800-2809.2003>.